1 Fast Iron Orbits in Stellarators

The basis of my work is an Orbit integrator providing initial condition for the interpolation. This work has already been done by Sergei Kasilov and Christopher Albert, who developed a fast routine, which integrates orbits in Fortran, called NEO. As I was rather new to plasma physics, and the code was not understandable for me, I decided to develop a routine in matlab myself and benchmark the results afterwards.

1.1 Single Particle Motion

To get an idea, what orbits of particles in Fusion devices look like, single particle motion is considered. That is to say that all interactions between particles are neglected. Also gravitation and the fields, which are induced by the moving charge (the particle we follow) are not taken into consideration.

1.2 Equations of Motion - Guiding Center Approach

To calculate the orbits of fast irons in stellarators one can start from the Lagrangian of a charged particle in an electromagnetic field. The trajectory of a charged particle in a magnetic field can be described by a superposition of fast gyromotion and motion of the point $\boldsymbol{R}$, which the particle is gyrating around. This point is called guiding center. Let us start from the Lagrangian 1.1, which treats the guiding center movement only, given by Helander and Sigmar, 2002.

$$\bar{L}(\boldsymbol{R}, \dot{\boldsymbol{R}}, t) = \frac{m_\alpha (\boldsymbol{b}(\boldsymbol{R}, t) \cdot \dot{\boldsymbol{R}})^2}{2} + Ze\boldsymbol{A}(\boldsymbol{R}, t) \cdot \dot{\boldsymbol{R}} - \mu B(\boldsymbol{R}, t) - Ze\Phi(\boldsymbol{R}, t) \quad (1.1)$$

$\boldsymbol{b}$ ... *magnetic field unit vector* μ ... *magnetic moment* m_α ... *α particle mass*
B ... *magnetic field magnitude* Φ ... *electric potential* Z ... *charge number*
A ... *electromagnetic potential* e ... *elementary charge*

The described superposition is valid as long as the motion of the guiding center perpendicular to a surface of constant magnetic field is small compared to the gyroradius. To be more precise the ratio ϵ (1.2) of gyroradius ρ and characteristic length L_B of the magnetic field B has to be small.

$$\epsilon = \frac{\rho}{L_B} << 1 \qquad with \qquad L_B = \frac{1}{|\nabla ln \boldsymbol{B}|} \quad (1.2)$$

When condition 1.2 is fulfilled and the guiding center approach 1.1 makes sense, also the magnetic moment μ is constant.

The equations of motion can be deduced by inserting the Lagrangian 1.1 into the Euler Lagrange Equation. However the procedure is simplified by first introducing a new variable-the component of the particle velocity parallel to the magnetic field $v_{||} = \boldsymbol{b} \cdot \dot{\boldsymbol{R}}$. Here $\boldsymbol{b}$ is the unit vector of the magnetic field. The right way to make the Lagrangian 1.1 dependent on the new variable $v_{||}$ is to build the phase space Lagrangian 1.3 following the procedure described by Littlejohn, 1983.

$$\bar{L}(\boldsymbol{R}, \dot{\boldsymbol{R}}, v_{||}, t) = (m_\alpha v_{||} \boldsymbol{b}(\boldsymbol{R}, t) + Ze\boldsymbol{A}(\boldsymbol{R}, t)) \cdot \dot{\boldsymbol{R}} - \frac{m_\alpha v_{||}^2}{2} - \mu B(\boldsymbol{R}, t) - Ze\Phi(\boldsymbol{R}, t) \quad (1.3)$$

Now the equations of motion 1.5 are derived by inserting the Lagrangian 1.3 into the Euler Lagrange Equation and introducing the modified vector Potential $\boldsymbol{A}^*$ (1.4) with the modified magnetic field $\boldsymbol{B}^*$ and the modified electric field $\boldsymbol{E}^*$ (1.4).

$$\begin{aligned}\boldsymbol{A}^*(\boldsymbol{R}, v_{||}, t) =& \boldsymbol{A}(\boldsymbol{R}, t) + \frac{m_\alpha v_{||}}{Ze}\boldsymbol{b}(\boldsymbol{R}, t)\\ \boldsymbol{B}^*(\boldsymbol{R}, v_{||}, t) =& \boldsymbol{\nabla} \times \boldsymbol{A}^*(\boldsymbol{R}, v_{||}, t)\\ \boldsymbol{E}^*(\boldsymbol{R}, v_{||}, t) =& eZ\left(\frac{\partial \boldsymbol{A}^*(\boldsymbol{R}, v_{||}, t)}{\partial t} - \boldsymbol{\nabla}\Phi(\boldsymbol{R}, t)\right)\end{aligned} \tag{1.4}$$

$$\begin{aligned}\dot{v_{||}} =& -\frac{\boldsymbol{B}^*(\boldsymbol{R}, v_{||}, t)\cdot(\mu\boldsymbol{\nabla}B(\boldsymbol{R}, t) - \boldsymbol{E}^*(\boldsymbol{R}, v_{||}, t)}{m_\alpha \boldsymbol{B}^*(\boldsymbol{R}, v_{||}, t)\cdot\boldsymbol{b}(\boldsymbol{R}, t)}\\ \dot{\boldsymbol{R}} =& \frac{Zev_{||}\boldsymbol{B}^*(\boldsymbol{R}, v_{||}, t) + \boldsymbol{b}(\boldsymbol{R}, t)\times(\mu\boldsymbol{\nabla}B(\boldsymbol{R}, t) - \boldsymbol{E}^*(\boldsymbol{R}, v_{||}, t)(\boldsymbol{R}, t))}{Ze\boldsymbol{B}^*(\boldsymbol{R}, v_{||}, t)\cdot\boldsymbol{b}(\boldsymbol{R}, t)}\end{aligned} \tag{1.5}$$

1.2.1 Normalization of the Equations of Motion

To make the representation of orbit variables clear and comparable the equations of motion 1.5 are normalized by their thermal velocity v. One wants to replace the parallel velocity $v_{||}$ by ${v_{||}}^n = \frac{v_{||}}{v}$, the magnetic moment μ by $\mu^n = \frac{\mu}{m_\alpha v^2}$ and the differential time element dt by $dt^n = v \cdot dt$. To make this variable transformation possible, the first equation of motion 1.5 has to be divided by v^2 and the second one by v. Additionally nominator and denominator of both equations are normalized by the magnetic field magnitude B. Introducing a new variable $\rho_0(\boldsymbol{R}, t) = \frac{m_\alpha v}{ZeB(\boldsymbol{R}, t)}$ and the modified unit vector $\boldsymbol{b}^*$ (see equation 1.6) results in the normalized equations of motion 1.7.

$$\boldsymbol{b}^*(\boldsymbol{R}, {v_{||}}^n, t) = \boldsymbol{b}(\boldsymbol{R}, t) + {v_{||}}^n\rho_0(\boldsymbol{R}, t)\boldsymbol{\nabla}\times\boldsymbol{b}(\boldsymbol{R}, t) \tag{1.6}$$

$$\begin{aligned}\frac{dv_{||}{}^{n}}{dt^{n}} &= -\frac{\boldsymbol{b}^{*}(\boldsymbol{R}, v_{||}{}^{n}, t)\cdot\left(\mu^{n}\boldsymbol{\nabla}B(\boldsymbol{R},t)-\frac{\boldsymbol{E}^{*}(\boldsymbol{R},v_{||},t)}{m_{\alpha}v^{2}B(\boldsymbol{R},t)}\right)}{\boldsymbol{b}^{*}(\boldsymbol{R}, v_{||}{}^{n}, t)\cdot\boldsymbol{b}(\boldsymbol{R},t)}\\ \frac{d\boldsymbol{R}}{dt^{n}} &= \frac{v_{||}{}^{n}\boldsymbol{b}^{*}(\boldsymbol{R}, v_{||}{}^{n}, t)+\boldsymbol{b}(\boldsymbol{R},t)\times\left(\mu^{n}\rho_{0}(\boldsymbol{R},t))\boldsymbol{\nabla}B(\boldsymbol{R},t)-\frac{\boldsymbol{E}^{*}(\boldsymbol{R},v_{||},t)}{eZvB(\boldsymbol{R},t)}\right)}{\boldsymbol{b}^{*}(\boldsymbol{R}, v_{||}{}^{n}, t)\cdot\boldsymbol{b}(\boldsymbol{R},t)}\end{aligned} \tag{1.7}$$

1.2.2 Equations of Motion in Curvilinear Coordinates

The magnetic field of a stellarator will be given in curvilinear coordinates. As the coordinate system does not have to be orthogonal in that case, covariant (lower index) and contravariant (upper index) vector components of the magnetic field will not be the same and a distinction has to be made D'haeseleer et al., 1991. As the scalar product is amongst others defined by $\boldsymbol{AB} = A_j B^j = A^j B_j$ the quantities in equation 1.4 and 1.5 are expressed cleverly by the concerning form 1.8, where $\sqrt{g}$ is the square root of the metric determinant being equal to the Jacobian.

$$\begin{aligned}\boldsymbol{\nabla}B &= \frac{\partial B}{\partial x^{\nu}}\boldsymbol{e}^{\nu}\\ \boldsymbol{b} &= \frac{B_{\nu}}{B}\boldsymbol{e}^{\nu}\\ \boldsymbol{b}\times\boldsymbol{\nabla}B &= \frac{1}{\sqrt{g}}\epsilon^{ij\nu}b_{j}\frac{\partial B}{\partial u^{i}}\boldsymbol{e}_{\nu}\\ \boldsymbol{B}^{*} &= B^{\nu}\boldsymbol{e}_{\nu}+\frac{m_{\alpha}v_{||}}{Ze\sqrt{g}}\epsilon^{ij\nu}\frac{\partial b_{j}}{\partial x^{i}}\boldsymbol{e}_{\nu}\end{aligned} \tag{1.8}$$

1.3 Magnetic Field

The magnetic field of the stellarator is calculated by the Variational Moments Equilibrium Code (VMEC) introduced by Hirshman and Whitson, 1983 . The magnetic field is evaluated in quasi-cylindrical coordinates (R, ϕ, Z), which are given by Fourier expansions of the so called VMEC coordinates (s, u, v) (see equation 1.9). Originally VMEC works in a left handed coordinate system. All quantities given in this chapter have been transformed to a right handed coordinate system by the variable transformation $u = -u_{\text{lefthanded}}$.

$$\begin{aligned} R(s,u,v) &= \sum_{m,n} R^{mn}(s)\cos(mu+nv) \\ Z(s,u,v) &= \sum_{m,n} Z^{mn}(s)\sin(mu+nv) \\ \lambda(s,u,v) &= \sum_{m,n} \lambda^{mn}(s)\sin(mu+nv) \end{aligned} \tag{1.9}$$

VMEC assumes nested flux surfaces, each which has constant pressure and is aligned parallel to the magnetic field (see figure 1.1). Coordinate s specifies the flux surface label, v is equivalent to the toroidal angle Φ and u corresponds to the poloidal angle which is chosen so that $u* = u + \lambda(s,u,v)$ leads to a coordinate system that makes the magnetic field lines straight. The most important feature of VMEC coordinates is that the Fourier Expansions (as f. e. 1.9) are symmetric in (u,v) and converge as quickly as possible. This is valid for u but not for $u*$.

The result of the VMEC field computation provides a great variety of quantities. In order to solve the equations of motion 1.5 the following are needed: Jacobian $\sqrt{g}$, magnetic field magnitude B, covariant components (B_s, B_u, B_v) -, and the contravariant components (B^u, B^v) of the magnetic field. Evaluation of these quantities can be done in two different ways.

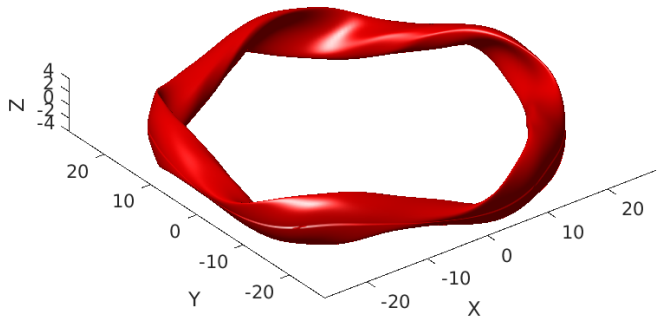

Figure 1.1: Outermost Stellarator Fluxsurface. The magnetic field is toroidally winded 5 times. VMEC output provides one of the five sections, the other 4 can be reproduced easily because of symmetry.

1.3.1 Evaluation of VMEC Coefficients in Matlab

The first way is straight forward and inspired by the VMECmatlab tool provided by Lanzerson, 2010. All of the needed quantities are described by an array of Fourier Coefficients (g^{mn}, B^{mn},...) . On the grid (or on the half grid s = 0.5, 1.5, 2.5, ...) of given flux surfaces they are evaluated in analogy to 1.10. Nevertheless to expand the quantities to whole space - eventually not covered by the VMEC flux surfaces, fast B Spline Interpolation of the evaluated quantities in the variable s is used. The unit magnetic field vectors are constructed by dividing each component by the magnetic field magnitude.

$$
\begin{aligned}
g(s,u,v) &= \sum_{m,n} g^{mn}(s)\cos(mu+nv) \\
B(s,u,v) &= \sum_{m,n} B^{mn}(s)\cos(mu+nv) \\
B_u(s,u,v) &= -\sum_{m,n} B^{umn}(s)\cos(mu+nv) \\
B_v(s,u,v) &= -\sum_{m,n} B^{vmn}(s)\cos(mu+nv) \\
B^s(s,u,v) &= -\sum_{m,n} {B_s}^{mn}(s)\sin(mu+nv) \\
B^u(s,u,v) &= -\sum_{m,n} {B_u}^{mn}(s)\cos(mu+nv) \\
B^v(s,u,v) &= -\sum_{m,n} {B_v}^{mn}(s)\cos(mu+nv)
\end{aligned}
\tag{1.10}
$$

Derivatives in u and v are done analytically by differentiating each sum component. In s the constructed spline is differentiated.

1.3.2 Construction from the Toroidal Flux

The second way to compute the magnetic field originates from the Fortran routine NEO. The trick is to start from straight field line coordinates * and compute the contravariant magnetic field component B^{v*} from the toroidal flux Φ_t, following relation 1.11 introduced by D'haeseleer et al., 1991. Keep in mind that the quantities marked with * are given in straight field line coordinates and differ from the ones given in VMEC coordinates. Further details on the concerning transformation are discussed below.

$$
B^{v*}(s,u,v) = \frac{\frac{\partial \Phi_t(s)}{\partial s}}{2\pi\sqrt{g^*(s,u,v)}} \tag{1.11}
$$

Subsequently the contravariant magnetic field component B^{u*} is determined by the rotational transform ι and B^{v*} (see equation 1.12) .

$$B^{u*}(s,u,v) = \iota(s)B^{v*}(s,u,v) \tag{1.12}$$

Toroidal flux $\Phi_t(s)$ and inverse rotational transform $\iota(s)$ are provided by VMEC, each expressed as a vector containing values on the concerning flux surfaces. As the toroidal flux is increasing linearly with s, its derivative is just a constant.
In the next step covariant components of the magnetic fields are calculated by 1.14 using the metric g^*. Calculation of the metric matrix components in VMEC coordinates g_{ij} is explained brilliantly by White, 2001 and quoted in equation 1.13. Again, keep in mind the transformation to straight field line coordinates *, which is explained below.

$$g_{ij}(s,u,v) = \frac{\partial R(s,u,v)}{\partial i} \cdot \frac{\partial R(s,u,v)}{\partial j} + \frac{\partial Z(s,u,v)}{\partial i} \cdot \frac{\partial Z(s,u,v)}{\partial j} + \delta_{iv}\delta_{jv}R^2(s,u,v) \tag{1.13}$$

$$\begin{aligned} {B_s}^* &= {g_{su}}^* B^{u*} + {g_{sv}}^* B^{v*} \\ {B_u}^* &= {g_{uu}}^* B^{u*} + {g_{uv}}^* B^{v*} \\ {B_v}^* &= {g_{vu}}^* B^{u*} + {g_{vv}}^* B^{v*} \end{aligned} \tag{1.14}$$

The magnetic field magnitude B is invariant under coordinate transformations and is given by the root of the scalar product of co- and contravariant magnetic field components 1.15.

$$B = \sqrt{B^{u*}{B_u}^* + B^{v*}{B_v}^*} \tag{1.15}$$

In the last step all quantities are transferred from straight field line coordinates to VMEC coordinates, to make them comparable. Derivatives in s, u and v are done numerically by the a first order finite differential method.

Coordinate Transformation

Basically for all conversions of quantities from the VMEC coordinate system to the straight field line coordinate system and back, the transformation matrix 1.16 is needed. From $s^* = s$, $u^* = u + \lambda(s,u,v)$ and $v^* = v$ the transformation matrix $(* \leftarrow)$ is built and its inverse $(\leftarrow *)$ is calculated.

$$\begin{aligned}(* \leftarrow) &= \begin{pmatrix} 1 & 0 & 0 \\ \frac{\partial\lambda}{\partial s} & 1+\frac{\partial\lambda}{\partial u} & \frac{\partial\lambda}{\partial v} \\ 0 & 0 & 1 \end{pmatrix} \\ (\leftarrow *) &= \frac{1}{1+\frac{\partial\lambda}{\partial u}} \cdot \begin{pmatrix} 1+\frac{\partial\lambda}{\partial u} & 0 & 0 \\ -\frac{\partial\lambda}{\partial s} & 1 & -\frac{\partial\lambda}{\partial v} \\ 0 & 0 & 1+\frac{\partial\lambda}{\partial u} \end{pmatrix}\end{aligned} \tag{1.16}$$

Scalar quantities like f. e. $\sqrt{g}$ can be back transformed by multiplication with the inverse transformation matrix determinant (see f. e. equation 1.17).

$$\sqrt{g^*} = \sqrt{g} \cdot \left|(\leftarrow *)\right| = \frac{\sqrt{g}}{1+\frac{\partial\lambda}{\partial u}} \tag{1.17}$$

Vectors like f. e. the contravariant magnetic field vector $\boldsymbol{B}^{c*}$ can be transformed by multiplication with the transformation matrix (see f. e. equation 1.18).

$$\boldsymbol{B}^c = (\leftarrow *) \cdot \boldsymbol{B}^{c*} \tag{1.18}$$

Matrices like f. e. the metric g can be back transformed by matrix multiplication of the inverse transformation matrix on both sides (see f. e. equation 1.19, where ^{T} indicates transpose).

$$g^* = (\leftarrow *)^T \cdot g \cdot (\leftarrow *) \tag{1.19}$$

1.3.3 Comparison of the two Approaches

The first approach to calculate the magnetic quantities (see subsection 1.3.2) was used to benchmark the NEO Code calculations in Fortran (see subsection 1.3.2). Jacobian $\sqrt{g}$, magnetic field magnitude B, covariant components (B_s, B_u, B_v) -, and contravariant components (B^u, B^v) of the magnetic field are plotted on randomly chosen points (u, v) over the fluxsurface label s, which is transformed to go from zero (innermost fluxsurface) to one (outermost fluxsurface). The outcomes of both routines agree quite well. One representative point $(u = 33, v = 97)$ is illustrated in figure 1.2.

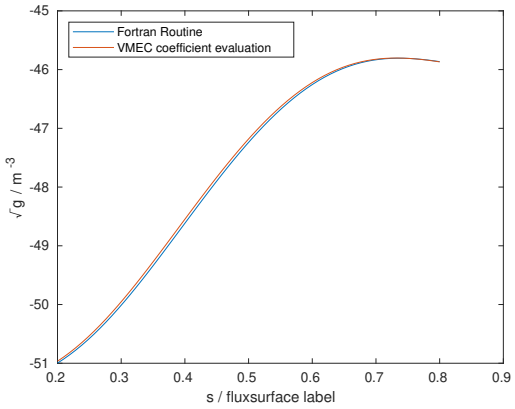

(a) Jacobian

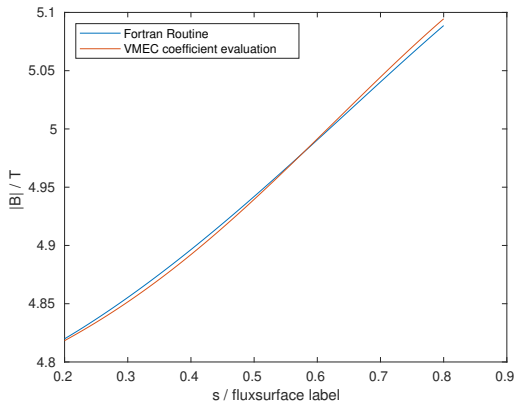

(b) magnetic field magnitude

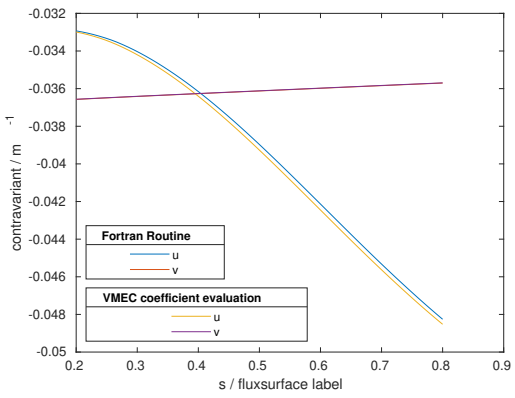

(c) contravariant components of $\boldsymbol{b}$

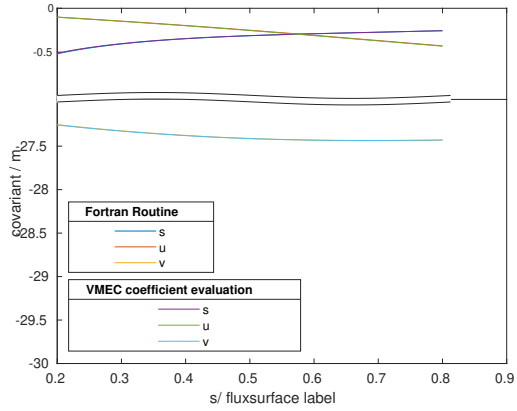

(d) covariant components of $\boldsymbol{b}$

Figure 1.2: comparison of magnetic quantities at $u = 0.33$ and $v = 0.97$

Note that the axis in figure 1.2d is broken, meaning that the covariant unit vector points nearly in toroidal direction v.

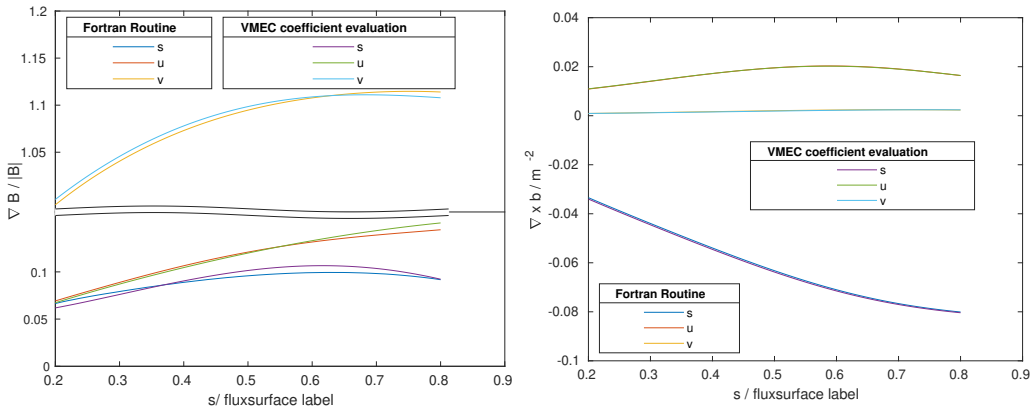

(a) covariant ∇B components

(b) contravariant $\nabla \times \boldsymbol{b}$ components

Figure 1.3: comparison of derivatives at $u = 0.33$ and $v = 0.97$

To guarantee the correctness of derivatives, the covariant gradient of the magnetic field ∇B and the contravariant curl of the unit magnetic field vector $\nabla \times \boldsymbol{b}$ calculated by both routines are compared in figure 1.3. Notice small deviations between the approaches in the gradient of the magnetic field magnitude 1.3a.

1.4 Orbit Integrator

1.4.1 Initial Conditions and Integration Parameters

Fast α - particles - the fusion products, initially have an energy of $E = 3.5\ MeV$. The thermal velocity of fast α particles is given by $v = \sqrt{\frac{2 \cdot E \cdot e}{m_\alpha}}$. The orbit shape depends on both the initial position and the normalized parallel velocity $v_{||}^n$ of the particle. In case of a high ${v_{||}}^n{}_p$ we expect the guiding center orbit to move along the magnetic field lines, resulting in a passing orbit. On the other hand a small ${v_{||}}^n{}_t$ means high perpendicular velocity, so that the mirror effect plays an important role and the particle will be reflected, resulting in a trapped orbit. In order to investigate both cases the alpha particle is placed somewhere inside the Stellarator and the orbit is computed for both cases ${v_{||}}^n{}_p$ and ${v_{||}}^n{}_t$. The modified electric field $\boldsymbol{E}^*(\boldsymbol{R}, {v_{||}}^n, t)$ is set to zero everywhere. Then the equations of motion 1.7 are solved by the matlab implemented ordinary differential equation solver ode45 with initial conditions given in table 1.1 . Normalized integration time t^n, absolute Tolerance $AbsTol$, and relative Tolerance $RelTol$ of the integrator are listed in the same table 1.1 for trapped and passing case.

s	u	v	${v_{||}}^n{}_p$	${v_{||}}^n{}_t$	t^n / m	AbsTol	RelTol
0.35	0.33	0.97	0.9	0.1	2.5e-5	1e-8	1e-12

Table 1.1: initial conditions and integration parameters

1.4.2 Resulting Orbits

First of all the normalized magnetic moment μ^n is observed over time (see figure 1.4) to monitor integration errors. Considerable changes indicate failure, because the magnetic moment is a constant of motion. In the passing case deviations of the magnetic moment are in the order of $1e-8$ and in the trapped case in the order of $1e-9$.

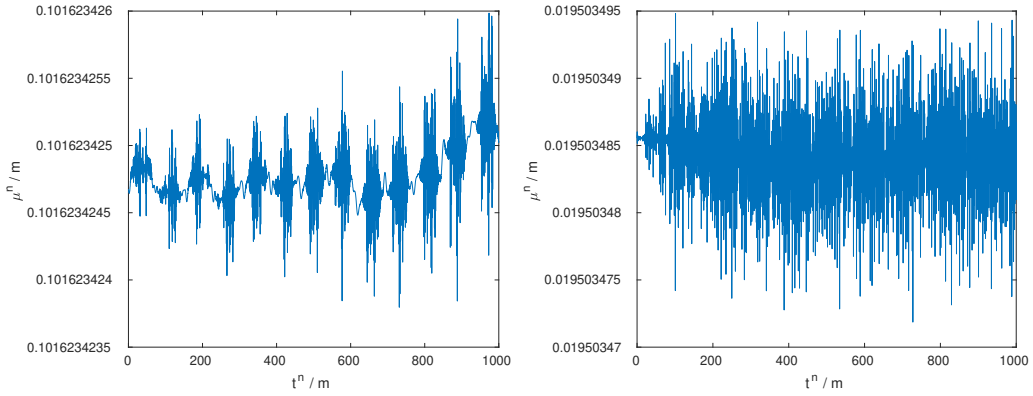

(a) trapped case (b) passing case

Figure 1.4: conservation of magnetic moment

The VMEC coordinates (s, u, v) of the alpha particle are given at every integration time step. For a better imagination of the particle movement, it is plotted for the trapped and passing case in three dimensional Cartesian space. In figure 1.5a and 1.5b one can easily see that in the passing case the particle follows the field line without changing direction, while the trapped particle is reflected many times. In addition, just the poloidal part of the movement is plotted in figure 1.5c andreffig:3dd.

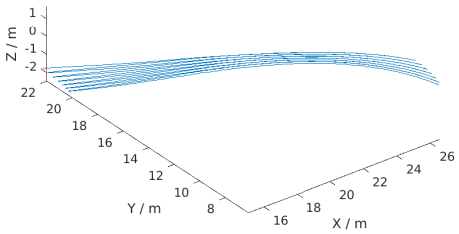

(a) trapped case: 3d

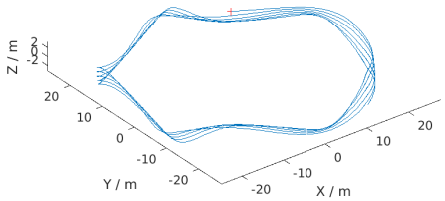

(b) passing case: 3d

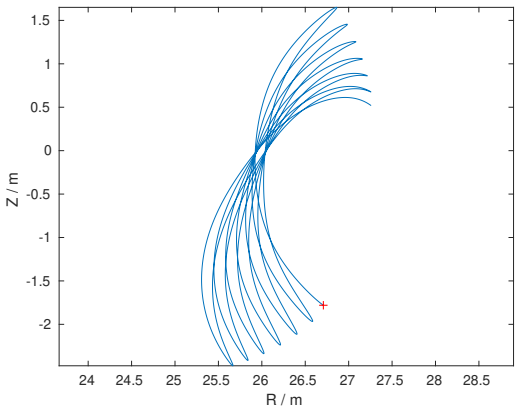

(c) trapped case: poloidal plane

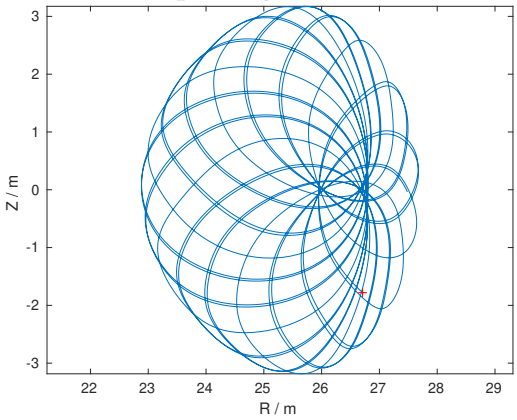

(d) passing case: poloidal plane

Figure 1.5: particle movement; starting point marked in red

1.4.3 Comparison of the Integrators

The matlab ode45 routine was used to benchmark the NEO Code calculations in Fortran (see subsection 1.3.2), equivalently working with an adaptable Runge Kutta method. In order to compare the results, initial conditions and integration parameters from table 1.1 were used for both routines. The integration variables s, u, v, and $v_{||}{}^{n}$ are graphically compared over time in figure 1.6 for the trapped case and in figure 1.7 for the passing case.

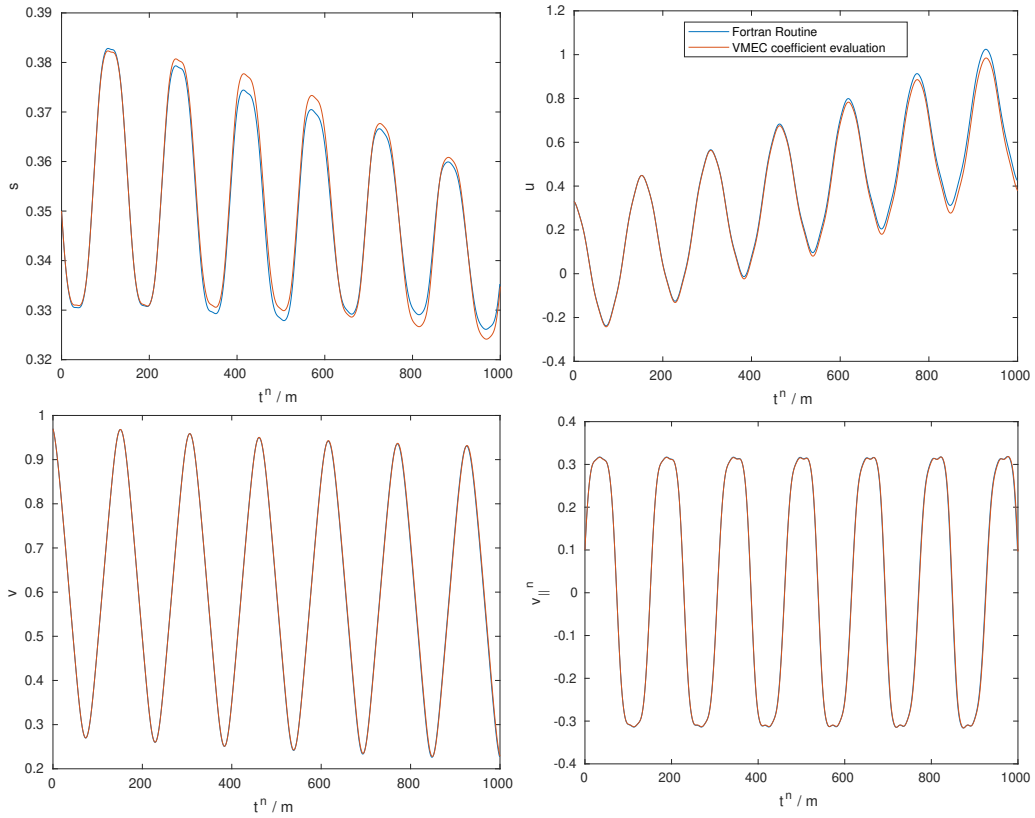

Figure 1.6: comparison of integration variables: trapped case

Deviations between the methods in variables s and u originate from the $\boldsymbol{b} \times \boldsymbol{\nabla} B$ term in equation 1.7, which have a more significant contribution in the trapped case. Small deviations in the gradient of the magnetic field

magnitude (see figure 1.3) due to different differentiation methods are notable mainly in s and u, because the covariant unit vector $\boldsymbol{b}$ points nearly in toroidal direction v.

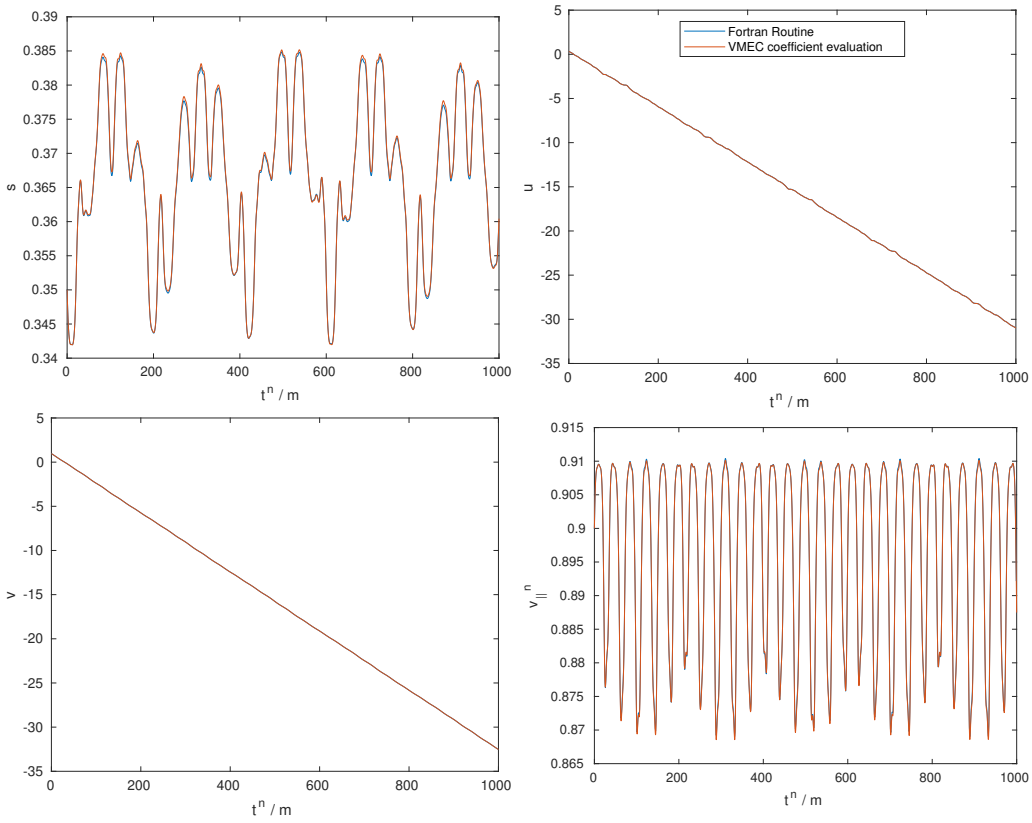

Figure 1.7: comparison of integration variables: passing case

Another important property of integrators is the computation time, which is listed for both cases and for both integrators in table 1.2. The Fortran Routine is obviously faster, which is the reason why it will be used in future calculations.

	matlab	Fortran
passing case	150 s	0.5 s
trapped case	120 s	0.5 s

Table 1.2: computation time of integrators

Bibliography

D'haeseleer, W. D. et al. (1991). Springer Verlag (cit. on pp. 4, 7).
Helander, P. and D. J. Sigmar (2002). Cambridge University Press (cit. on p. 1).
Hirshman, S. P. and J. C. Whitson (1983). "Steepest-decent moment method for three-dimensional magnetohydrodynamic equilibria." In: *Phsy. Fluids* 26 (cit. on p. 5).
Lanzerson, Samuel (2010). *matlabVMEC*. https://es.mathworks.com/matlabcentral/fileexchange/2903 matlabvmec (cit. on p. 6).
Littlejohn, R. G. (1983). "Variational principles of guiding centre motion." In: *J. Plasma Physics* 29.1, pp. 111–125 (cit. on p. 2).
White, Roscoe B. (2001). 2. Danvers, USA: ICP. Chap. 2. ISBN: 1-86094-277-6 (cit. on p. 8).